SUPPORTING INFORMATION

Revisiting Significance on Kinetic Inertia in Complex formation/decomplexation of Metal-ATCUN Peptide Complex.

Valentina Borghesani*[a], Aleksandra Anna Bonini[a], Matteo Tegoni[a]

Table of contents:

1. MATERIALS

GGH-Pep (GGHWGKRG-Am) and **AAH-Pep** (AAHAWG-Am) were synthesised (see section below). MBHA rink-amide (rink amide methylbenzhydrylamine) resin was purchased from IRIS Biotech, Fmoc protected amino acids and other reagents for peptide synthesis, were purchased from CEM Corporation. All other chemicals were purchased from Merck and used without further purification.

2. EXPERIMENTAL PROCEDURES

2.1. Peptide synthesis

GGH-Pep and **AAH-Pep** were synthesized according to published methods[1,2] using standard Fmoc chemistry solid-phase peptide synthesis on a rink amide resin (MBHA) with a Liberty Blue 2.0 (CEM Corporation). Fmoc-amino acids (4-fold excess) were sequentially coupled to the growing peptide chain using DIC/Oxyma Pure (N,N'-diisopropylcarbodiimide / Ethyl cyano(hydroxyimino)acetate) as activating mixture by microwave assisted peptide synthetizer. DIC/Oxyma mixture was chosen instead than more classical DIEA/HBTU(N,N-Diisopropylethylamine / N,N,N′,N′-Tetramethyl-O-(1H-benzotriazol-1-yl)uronium hexafluorophosphate) activating mixture since HBTU, as all the uranium based coupling agents, could induce airborne allergic skin sensitization or induce anaphylaxis.[3,4] Deprotection of Fmoc was carried out with a 10% piperidine/N,N-dimethylformamide and 0.1M of Oxyma, to prevent degradation or racemization during synthesis.[5,6] Peptides were simultaneously cleaved and deprotected using a cleavage cocktail of trifluoroacetic acid (TFA), triisopropilsilane (TIS), H2O (95:2.5:2.5 TFA:TIS:H2O) for 2.5 h at room temperature, 10 mL cleavage cocktail per 0.2 g of resin.[7] After filtration of the resin, the solvent was concentrated under nitrogen flow. The peptides were precipitated with ice-cold diethyl ether, recovered by vacuum filtration. Crude peptides were dissolved in acetonitrile:H2O 1:1 and purified by preparative reversed-phase HPLC using a Agilent 1260 Infinity II HPLC system with a Jupiter column C18 (250 × 50 mm, 300 A, 15 µm spherical particle size, Phenomenex). Flow rate 10 ml/min with a mobile phase containing solvent A (water in 0.1% TFA), and a linear gradient from 10 to 70% of solvent B (acetonitrile in 0.1% TFA) over 25 min for the elution of peptides.
LC-ESI-MS analyses to assess peptides purity were performed. Trace profiles and ESI mass spectra associated are reported in Figure S1 and S2.

2.2. Stock solutions

Stock solutions (ca. 1.5-2.0 mM) of **GGH-Pep** and **AAH-Pep** were prepared by weight in doubly distillated water. The concentration of peptide was determined by UV-Visible absorption based on the tryptophan absorbance at 280 nm (ε = 5690 M^{-1} cm^{-1}).[8–10] All spectroscopic experiments were performed in 50 mM Hepes buffer at pH 7.4, unless otherwise indicated.
Aqueous HEPES buffer solutions (50 mM, pH 7.4) were prepared in doubly distilled water.
Stock solutions of $CuCl_2$ and $NiCl_2$ were prepared by weight from analytical grade metal salts and standardized by ICP-MS.

2.3. Potentiometric titrations

Stability constants for the proton as well as Cu(II) and Ni(II) complexes of the **GGH-Pep** and **AAH-Pep** peptide were calculated from the pH-metric titration curves obtained under an nitrogen atmosphere (in order to avoid carbonates appearance into the sample) over the pH range 3.0−11.0 at 298.2 K and ionic strength of 0.1 M KCl using a total volume of 1.5 mL.
Potentiometric titrations were carried out using an automatic potentiometric Metrohm OMNIS titrator equipped with a semi-micro analogic glass electrode (Metrohm). The thermostabilized glass cell was equipped with a magnetic stirring system, a microburette delivery tube, and an inlet-outlet tube for nitrogen. Solutions were titrated with 0.04917 M carbonate-free KOH; previously standardized against potassium hydrogen phthalate.11 The electrodes were calibrated daily in terms of [H+] by titrating HCl with KOH under the same experimental conditions as mentioned above. Electrode parameters were determined using the Gran's method 11 and pKw value resulted to be 13.76.
The peptide concentration was 0.267 mM, and the metal ion to ligand molar ratio was 1:1.2 (Cmetal = 0.222 mM). Protonation and stability complex constant calculations were performed using HyperQuad 2013 software.12 Standard deviations were calculated by HyperQuad 2013 and refer to random errors only. The distribution and competition diagrams were computed with the Hyss2009 program.13
In order of obtainment of the equilibrium through pH measurements vs. time different methods were applied by changing equilibration time before each potential measurement. Method conditions are detailed in Table S1.

Table S1. Potentiometric conditions. All samples are in aqueous solution (T = 298.2 K, *I* = 0.1 M in KCl).

Method	Signal drift (mV/min)	Minimum equilibration time (sec)	Maximum equilibration time (sec)	Volume addition (µL)
METHOD #1	1.0	10	300	1
METHOD #2	1.0	60	700	2
METHOD #3	1.0	120	900	2

Method #1 represented by minimum equilibration time of 10 sec and maximum equilibration time of 300 sec for each addition of 1 µL. It was changed to increase the minimum equilibration time at 60 sec and maximum equilibration time at 700 sec (Method #2). Increasing equilibration time the number of point collectable have been halved (volume increment: 2 µL). Since a significative improvement of the potentiometric curve has been observed, the equilibration time between each addition and its corresponding f.e.m. measure has been increased. In Method #3 after each addition a minimum of 120 sec and a maximum of 900 sec was waited before f.e.m. registration. As in Method #2 the number of points collected was halved respect to Method #1.

2.4. Spectroscopic studies

2.4.1. UV-Visible.

UV-Visible titration experiments were carried out at 298.2 K on a Cary3500 spectrophotometer provided with a Peltier thermostat, using 1 cm path length black quartz cuvettes. Samples of **GGH-Pep** were prepared in 50 mM HEPES at pH 7.4 to obtain 0.3 mM final concentration. Spectrophotometric titrations were carried out by adding $CuCl_2$ or $NiCl_2$ to sample solutions up to ligand:metal ratio of 1:1.5 for **GGH-Pep** peptide. All titrations were performed in duplicate. With Cu(II), equilibration time of 2 min was waited after each addition. In the case of Ni(II), titrations were carried out with different equilibration times (5, 10, 15 minutes and overnight).

Kinetic metal complex formation at pH 7.4 in presence of Ni(II) or Cu(II) at ratio metal:peptide 1:1.2 were carried out. Kinetic metal complex formation in proximity of potentiometric spike (0.25 pH unit before and 0.25 pH unit after) at ratio metal:peptide 1:1.2 were carried out (pH 4 for Cu(II):**GGH-Pep** complexation and pH 7 for Ni(II):**GGH-Pep** complexation).

2.4.2. Circular dichroism (CD).

CD titration experiments were carried out with a Jasco J1500 spectropolarimeter equipped with a Peltier thermostat at 298.2 K, using 1 cm path length black quartz cuvettes. Samples **GGH-Pep** were prepared in 50 mM HEPES at pH 7.4 at 0.3 mM final peptide concentration. CD titrations were carried out by adding $CuCl_2$ or $NiCl_2$ to sample solutions up to ligand:metal ratio of 1:2 for **GGH-Pep** peptide. All titrations were performed in duplicate.
To investigate kinetic complex formation spectrophotometric titrations in presence of Ni(II) were carried out at different time intervals after metal addition, that is 5, 10 and 15 minutes, and on overnight-incubated batch samples.

2.4.3. Fluorescence spectroscopy

Fluorescence emission spectra were recorded at 298.2 K with an Edinburgh FLS1000 spectrofluorimeter with λ_{exc}=280 nm and λ_{em}=290-450 nm. The excitation and emission wavelength allow to observe the excitation and emission of the indolic fluorophore of Trp. Spectrofluorimetric titrations of **GGH-Pep** were carried out in aqueous buffer (50 mM HEPES, pH 7.4) using peptide solution at 10 µM. Each solution was titrated with $CuCl_2$ or $NiCl_2$ up to a metal:ligand ratio of ca. 12. All titrations were performed in duplicate. To investigate kinetic complex formation spectrophotometric titrations in presence of Ni(II) were carried out at different time intervals after metal addition, that is 5, 10 and 15 minutes, and on overnight-incubated batch samples. Due to faster Cu(II) complexation at pH 7.4, spectra were acquired only after 2 minutes of equilibration time.

3. Supporting Information Figures

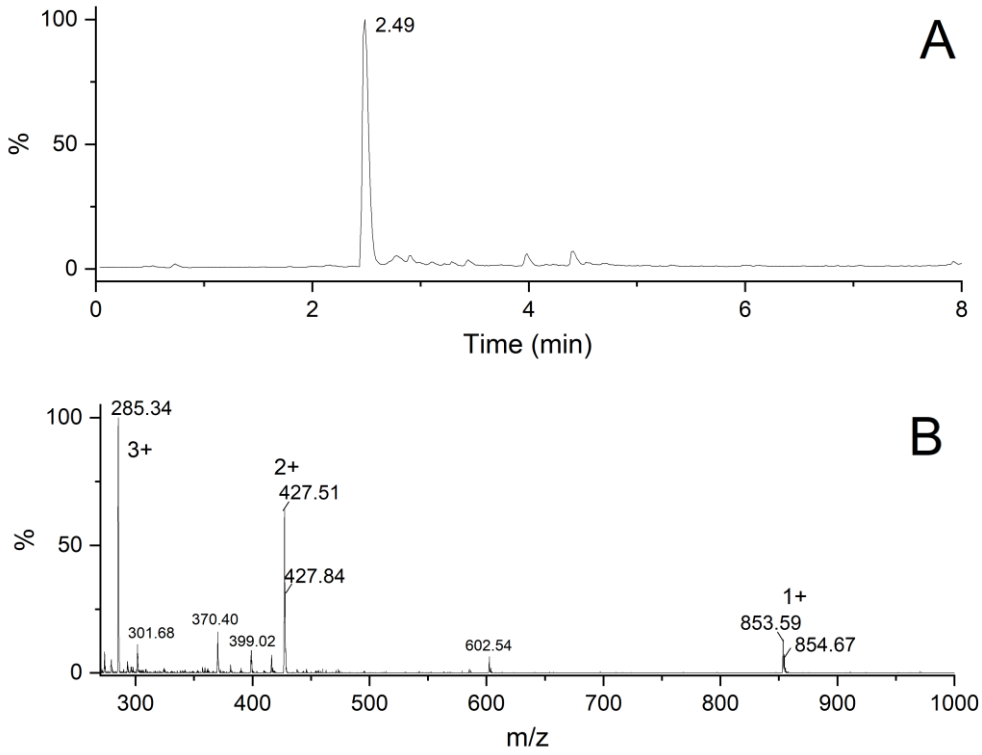

Figure S1.LC-MS chromatograms (A) and mass spectra of the peak at retention time 2.49 minutes (B) of the pure **GGH-Pep** peptide obtained by Solid Phase Peptide Synthesis and HPLC purification. Calculated $[M+H]^{+}$: 853.9, $[M+2H]^{2+}$: 427.5, $[M+3H]^{3+}$: 285.2; Found $[M+H]^{+}$: 853.6, $[M+2H]^{2+}$: 427.5, $[M+3H]^{3+}$: 285.3.

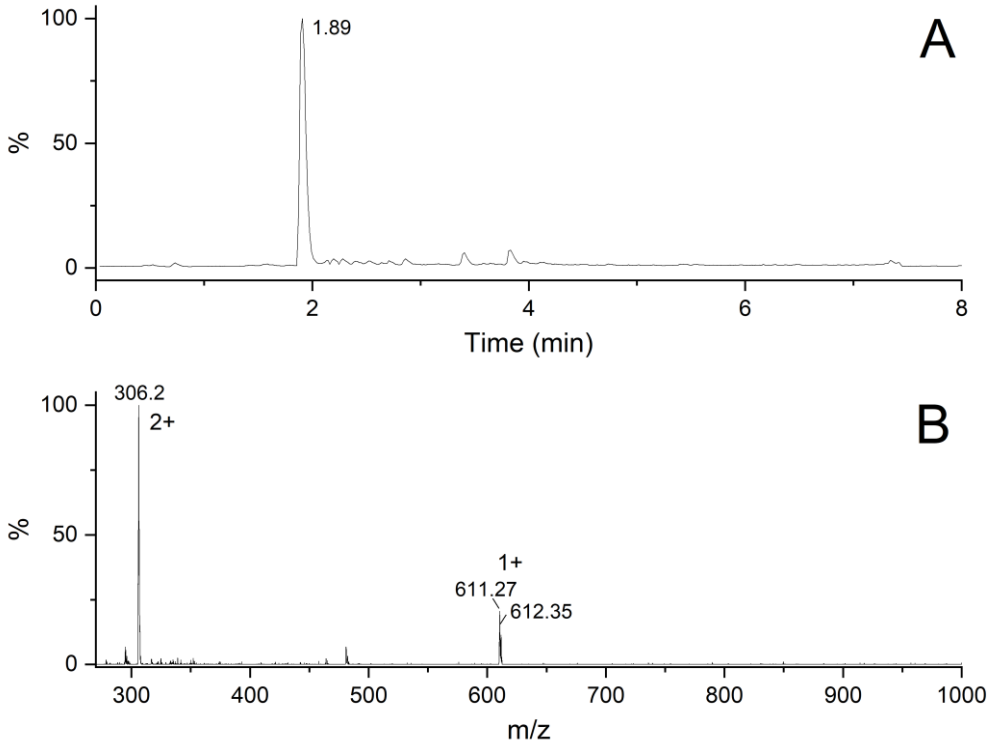

Figure S2. LC-MS chromatograms (A) and mass spectra of the peak at retention time 2.49 minutes (B) of the pure **AAH-Pep** peptide obtained by Solid Phase Peptide Synthesis and HPLC purification. Calculated $[M+H]^{+}$: 611.3, $[M+2H]^{2+}$: 306.1; Found $[M+H]^{+}$: 611.29, $[M+2H]^{2+}$: 427.5, $[M+3H]^{3+}$: 306.2.

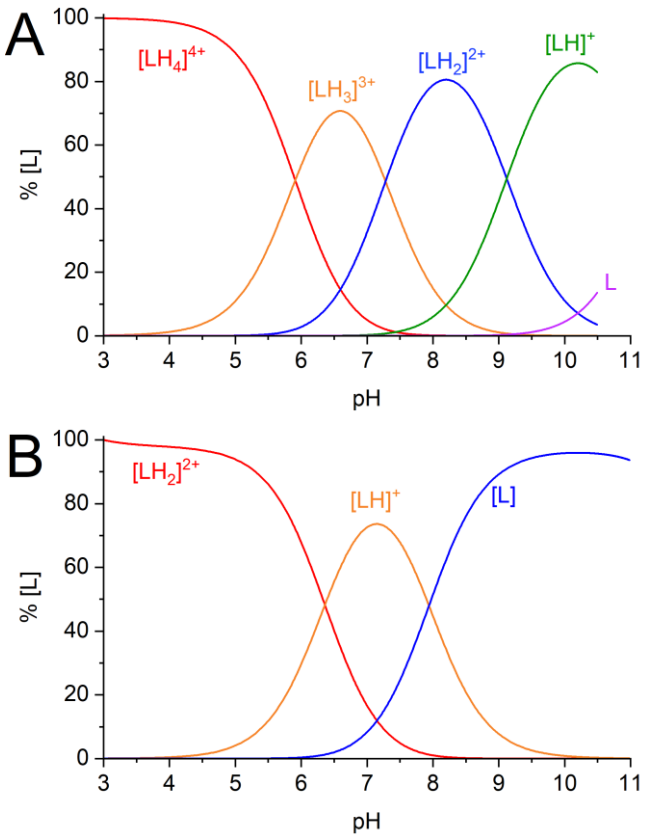

Figure S3. Representative distribution diagram of the protonation states of **GGH-Pep** (A) and **AAH-Pep** (B) in aqueous solution (C_{PepXXH} = 0.3 mM, I = 0.1 M (KCl), T = 298.2 K).

Table S2. Proton dissociation constants (pKa) of the fully protonated **AAH-Pep** peptide (H_2L^{2+}), and logarithms of overall formation constants (Log β) and acid dissociation constants (pK_a) of the copper(II) and nickel(II) complexes of **AAH-Pep** in aqueous solution (T = 298.2 K, I = 0.1 M in KCl). Standard deviations are given in parenthesis. L represents the completely deprotonated form of the peptide.

Species	Log β		pK_a	Dissociation site	Log β Perinelli et *al.* [14]		pK_a Perinelli et *al.* [14]
$[LH]^+$	7.9(1)		7.9	NH_3^+ N-terminal	7.94(1)		7.94
$[LH_2]^{2+}$	14.30(3)		6.4	$N_{im}H^+$ His	14.30(1)		6.36
$[CuLH_{-2}]$	-0.36(2)		8.81(9)	--	-0.47(1)		11.59
$[CuLH_{-3}]^-$	-9.17(9)		--	--	-12.06(3)		--
$[NiLH_{-2}]$	-7.37(5)		8.8(3)	--	nd		nd
$[NiLH_{-3}]^-$	-16.1(3)		--	--	nd		nd

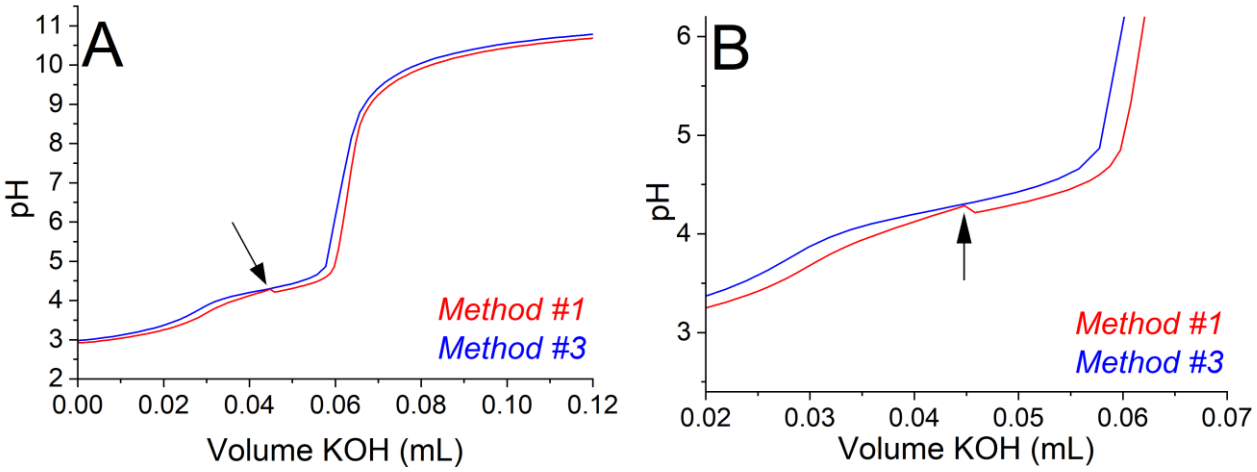

Figure S4. Potentiometric titration curve of **Copper(II)-GGH-Pep** complex. Arrow indicates the spike observed in around pH 4, caused by sudden H^+ concentration increment despite KOH additions ([KOH] = 0.04917 M; $C_{GGH\text{-}Pep}$ = 0.3 mM, I = 0.1 M (KCl), T = 298.2 K). Red curve: Method #1; blue curve: Method #3 (titration parameters are reported in Table S1).

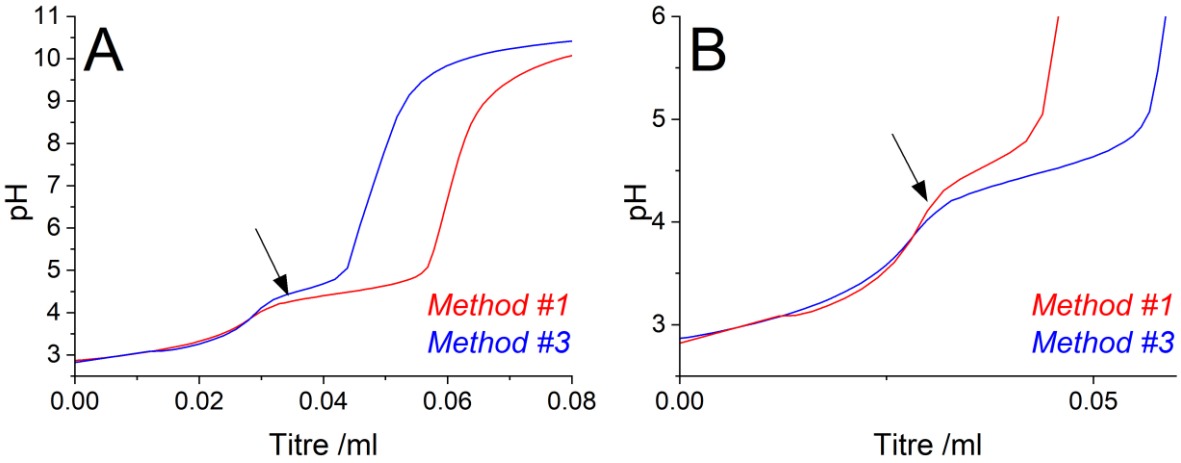

Figure S5. Potentiometric titration curve of **Copper(II)-AAH-Pep** complex. Arrow indicates the slope anomaly observed in around pH 4, caused by sudden H^+ concentration increment despite KOH additions ([KOH] = 0.04917 M; $C_{GGH\text{-}Pep}$ = 0.3 mM, I = 0.1 M (KCl), T = 298.2 K). Red curve: Method #1; blue curve: Method #3 (titration parameters are reported in Table S1).

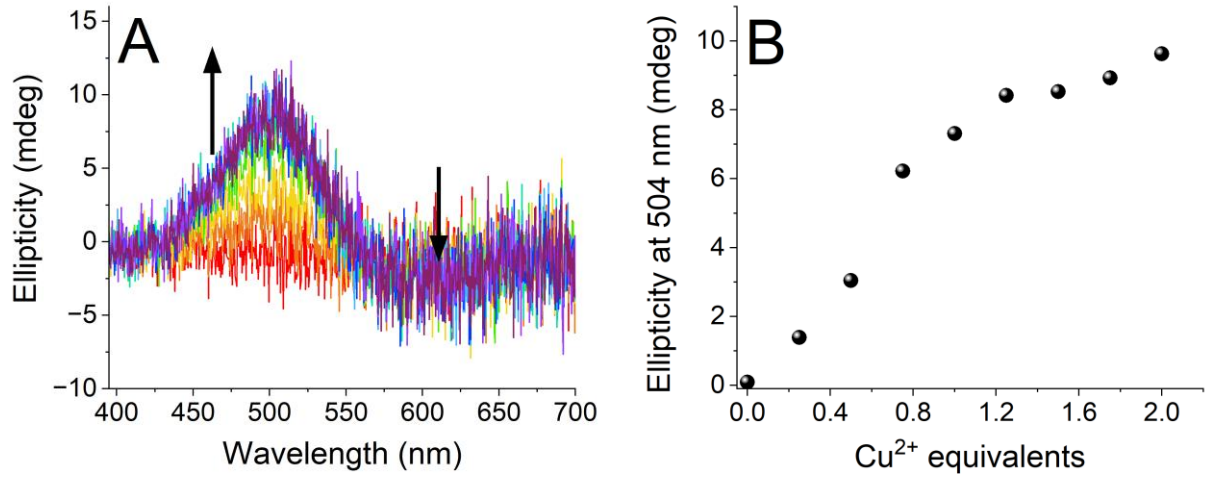

Figure S6 (A) CD spectra for the titration **GGH-Pep** with **Cu(II).** Cu(II): peptide = 0 (red spectrum) to 2 (purple spectrum), with 0.25 eq. additions. (B) Ellipticity at 504 nm as function of copper(II) equivalents. ($C_{GGH\text{-}Pep}$ = 0.3 mM, 50 mM HEPES pH 7.4, T = 25 °C)

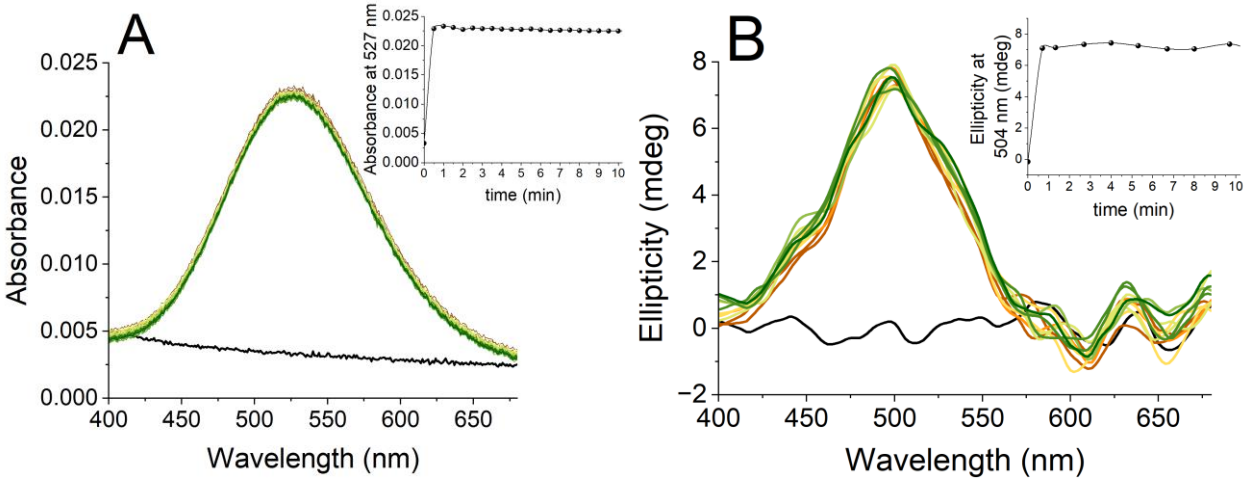

Figure S7. Kinetics of **Copper(II)-GGH-Pep** complex formation monitored by UV-Visible (Panel A) and CD (Panel B) spectrophotometry. (A) UV-vis spectra and kinetic profile at 527 nm (inset). (B) CD spectra and kinetic profile at 504 nm (inset). ($C_{GGH\text{-}Pep}$ = 0.3 mM, Cu(II):**GGH-Pep** 1:1.2, 50 mM Hepes pH 7.4, T = 298.2 K).

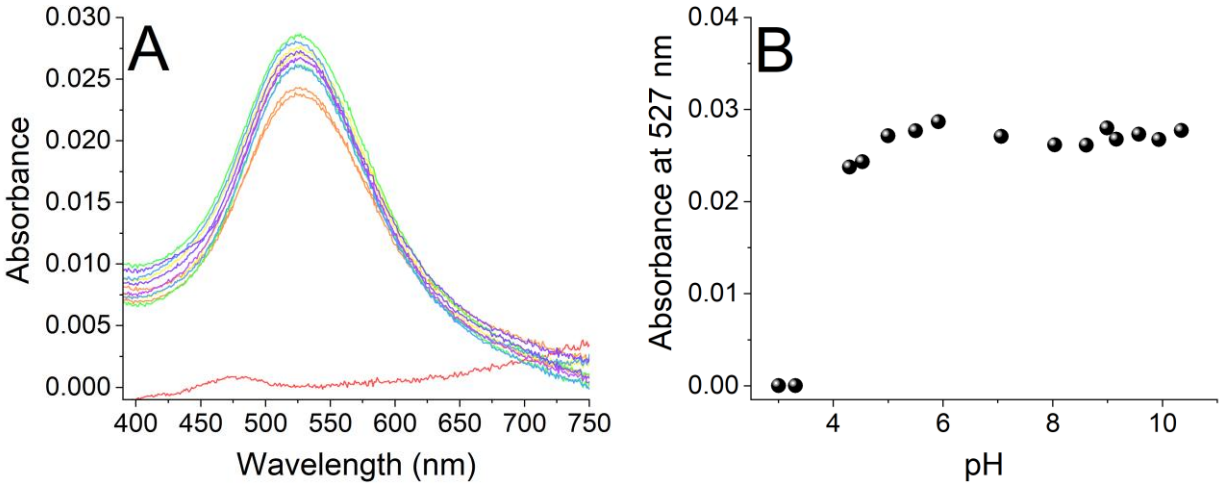

Figure S8. **Copper(II)-GGH-Pep** complex formation monitored by UV-Visible spectrophotometry as function of pH (Panel A) and absorbance at 527 nm as function of pH (Panel B). ($C_{GGH\text{-}Pep}$ = 0.3 mM, Cu(II):**GGH-Pep** 1:1.2, I = 0.1 M (KCl), T = 298.2 K). Spectra in red are at pH lower than 4, spectra in orange are at pH around 5, spectra in blue, purple and green are the spectra between pH 5 and 11.

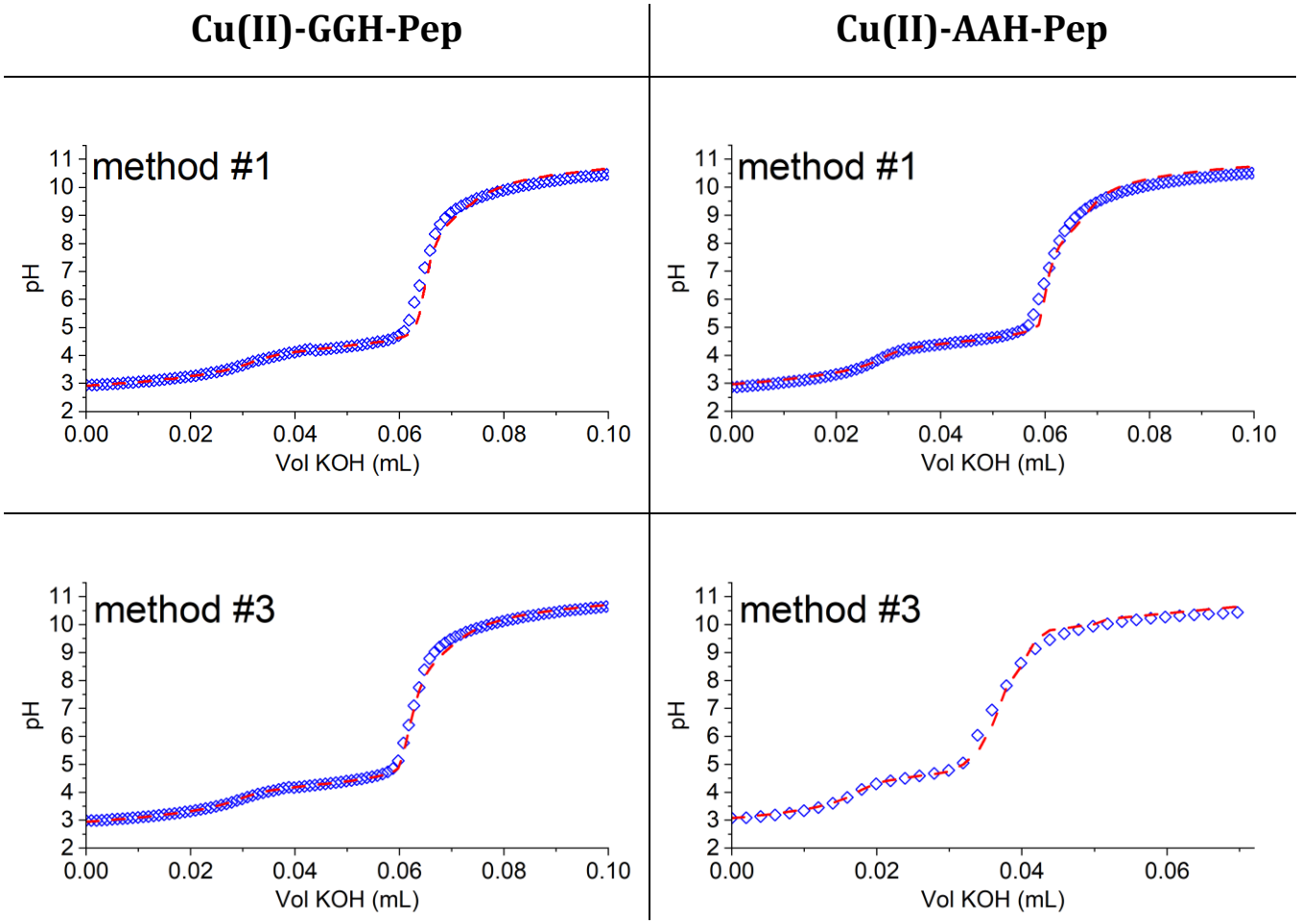

Figure S9. Potentiometric titration curve for complex-formation of **Copper(II)-GGH-Pep** and **Copper(II)-AAH-Pep** acquired with Method #1 and Method #3 at T = 298.15 K and I = 0.1 M (KCl). (Cu(II):Pep = 1:1.2, [Pep] = 0.3 mM, [Ni(II)]= 0.25 mM; KOH] = 0.04917 M). Blue diamonds: experimental data, red dotted line: fitting of potentiometric curve with the speciation model obtained with Method #3. Comparison of the pK_a obtained are reported in Table S3.

Table S3. Logarithms of overall formation constants (Log β) and acid dissociation constants (pK_a) of the **Copper(II)** complexes of **GGH-Pep** and **AAH-Pep** in aqueous solution (T = 298.2 K, I = 0.1 M in KCl) obtained with reliable speciation model based on long equilibration time (Method #3) and underestimates constants which would otherwise be obtained without long enough equilibration time (Method #1). Standard deviations are given in parenthesis. L represents the completely deprotonated form of the peptide, and H_4L^{4+} the fully protonated **GGH-Pep** peptide and H_2L^{2+} the fully protonated **AAH-Pep** peptide.

		Potentiometric curve with spike (**Method #1**)				Reliable potentiometric curve (**Method #3**)		
GGH-Pep	Species	Log β		pK$_a$		Log β		pK$_a$
	$[CuL]^{2+}$	20.02(3)		**9.1(1)**		20.04(4)		**8.8(2)**
	$[CuLH_{-1}]^{+}$	10.9(1)		--		11.2(2)		--
AAH-Pep	Species	Log β		pK$_a$		Log β		pK$_a$
	$[CuLH_{-2}]$	0.18(11)		**8.5(2)**		-0.36(2)		**8.81(9)**
	$[CuLH_{-3}]^{-}$	-8.1(5)		--		-9.17(9)		--

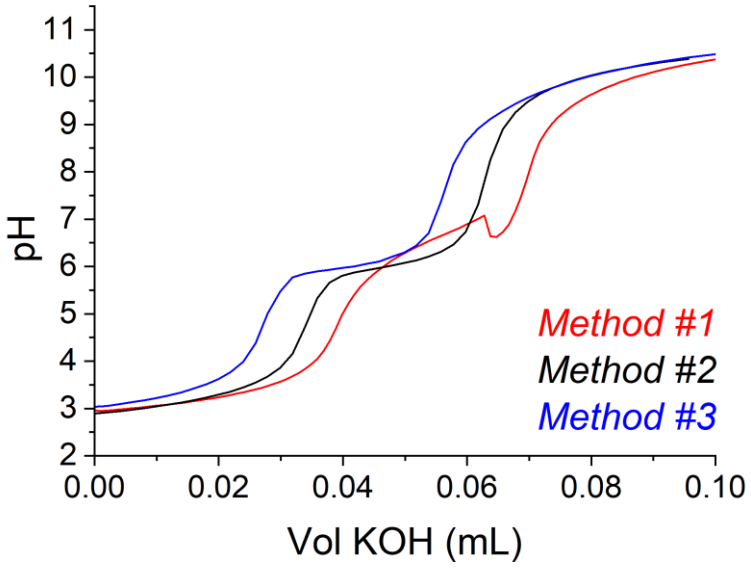

Figure S10 Potentiometric titration curve of **Nickel(II)-GGH-Pep** complex. Around 0.07 mL of KOH a significant spike caused by sudden H^+ concentration increment despite KOH additions can be observed in the red curve. ([KOH] = 0.04917 M; $C_{GGH\text{-}Pep}$ = 0.3 mM, I = 0.1 M (KCl), T = 298.2 K). Red curve: Method #1; black curve: Method #2, blue curve: Method #3 (titration parameters are reported in Table S1).

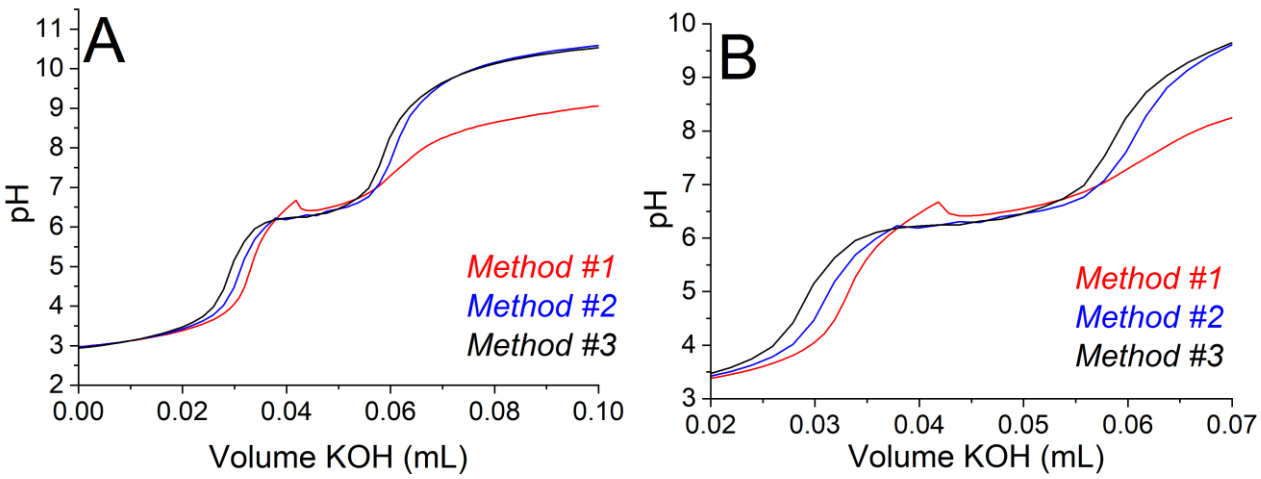

Figure S11 Potentiometric titration curve of **Nickel(II)-AAH-Pep** complex (A) and its zoom (B). Around 0.04 mL of KOH a significant spike caused by sudden H^+ concentration increment despite KOH additions can be observed in the red curve. ([KOH] = 0.04917 M; $C_{AAH\text{-}Pep}$ = 0.3 mM, I = 0.1 M (KCl), T = 298.2 K). Red curve: Method #1; blue curve: Method #2, black curve: Method #3 (titration parameters are reported in Table S1).

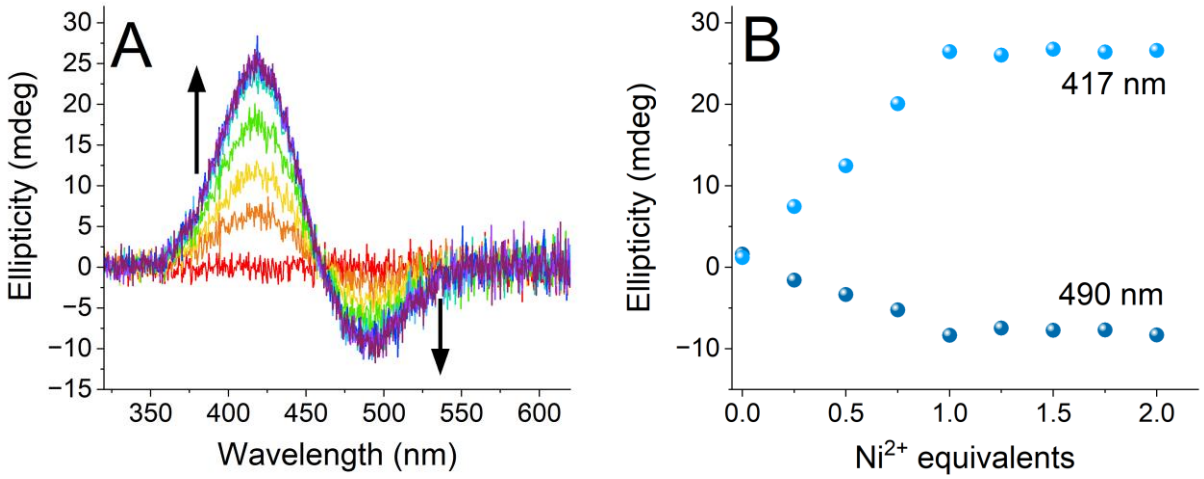

Figure S12 (A) CD spectra for the titration **GGH-Pep** with **Ni(II).** Ni(II): peptide = 0 (red spectrum) to 2 (purple spectrum), with 0.25 eq. additions. (B) Ellipticity at 417 nm and 490 nm as function of Nickel(II) equivalents. ($C_{GGH\text{-}Pep}$ = 0.3 mM, 50 mM HEPES pH 7.4).

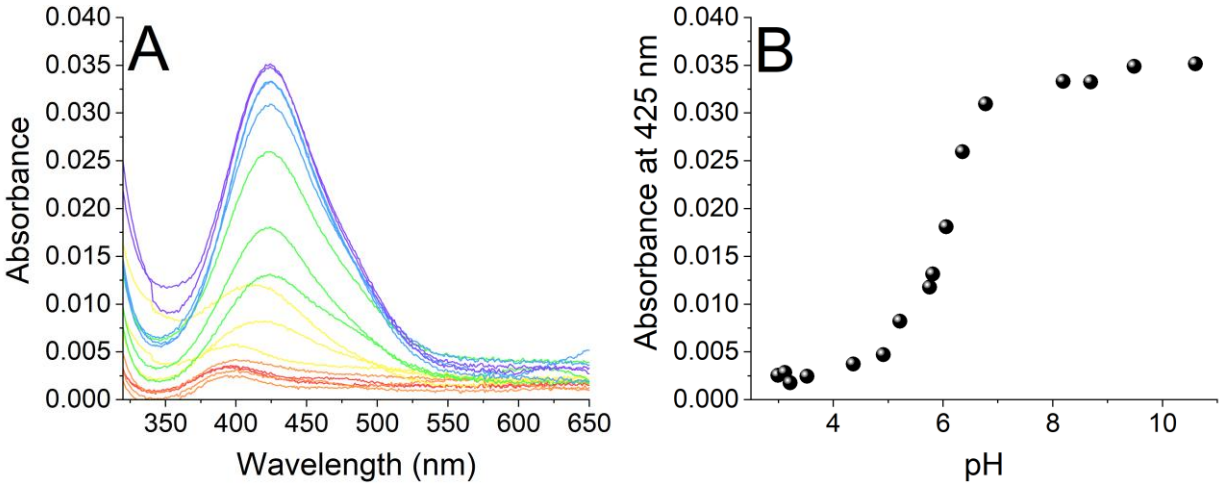

Figure S13. Nickel(II)-GGH-Pep complex formation monitored by UV-Vis spectrophotometry as function of pH (A) and absorbance at 425 nm as function of pH (B). ($C_{GGH\text{-}Pep}$ = 0.3 mM, Ni(II):**GGH-Pep** 1:1.2 , *I* = 0.1 M (KCl), T = 298.2 K).

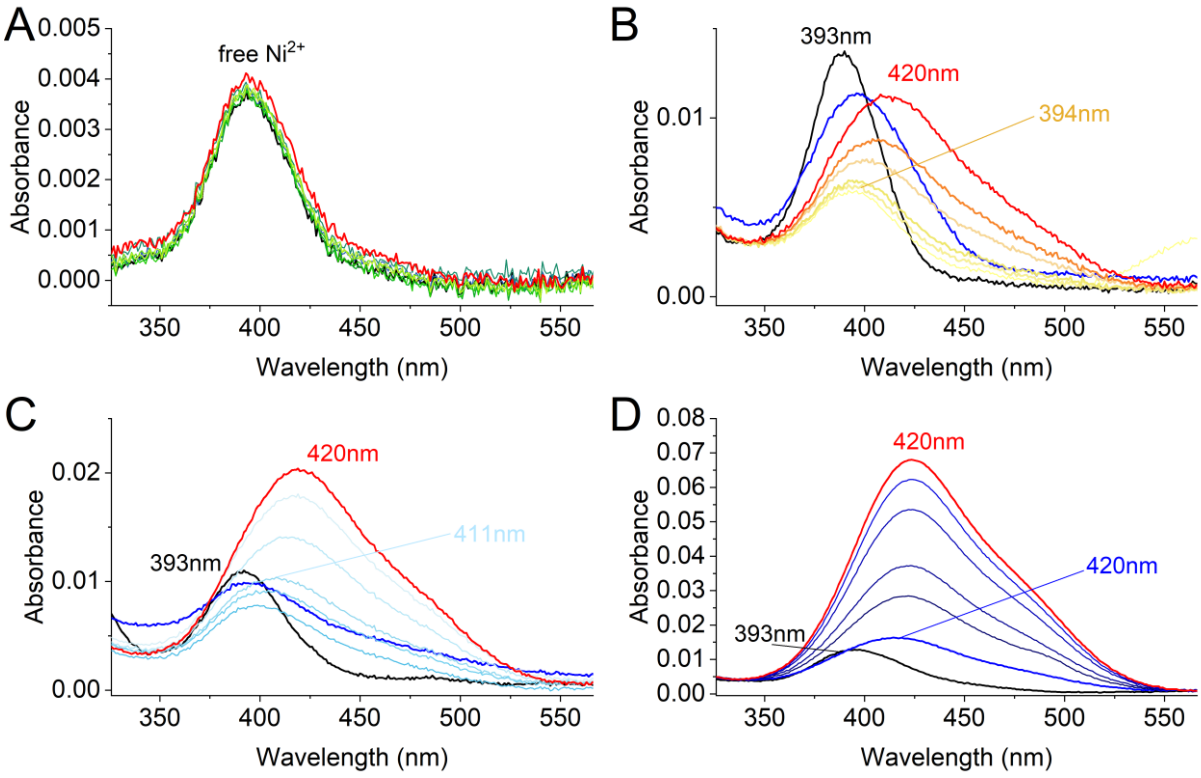

Figure S14. Kinetic of **Nickel(II)-GGH-Pep** complex formation monitored by UV-Vis spectrophotometry at pH 6.25 (A), 6.5 (B), 6.75 (C) and pH 7.4. ($C_{GGH\text{-}Pep}$ = 0.8 mM, $C_{Ni(II)}$ = 0.72 mM Ni(II):**GGH-Pep** 1:1.2, T = 298.2 K). In black t=0 after Ni(II) addition, in blue t=15s after Ni(II) addition and in red t=300s after Ni(II) addition.

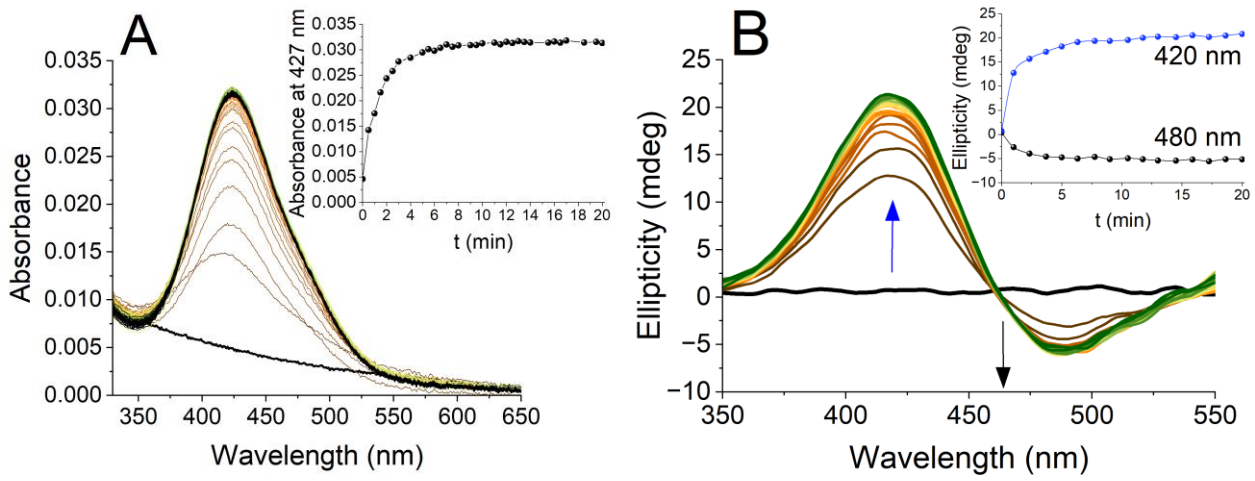

Figure S15 Kinetics of Nickel(II)-**GGH-Pep** complex formation monitored by UV-Vis and CD spectrophotometry at physiological pH. (A) UV-Vis spectra and kinetic profile at 427 nm (inset). (B) CD spectra and kinetic profile at 420 nm and 480 nm (inset) ($C_{\mathbf{GGH\text{-}Pep}}$ = 0.3 mM, Ni(II):**GGH-Pep** 1:1.2 , 50 mM Hepes pH 7.4, T = 298.2 K).

Ni(II)-GGH-Pep	Ni(II)-AAH-Pep
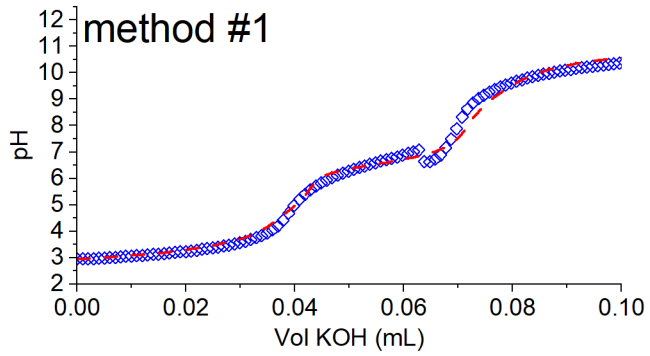	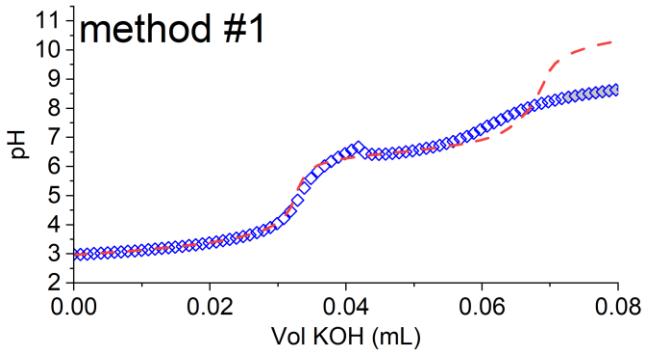 fitting not reliable
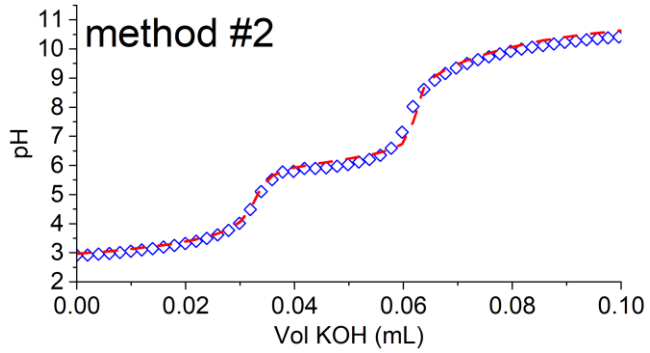	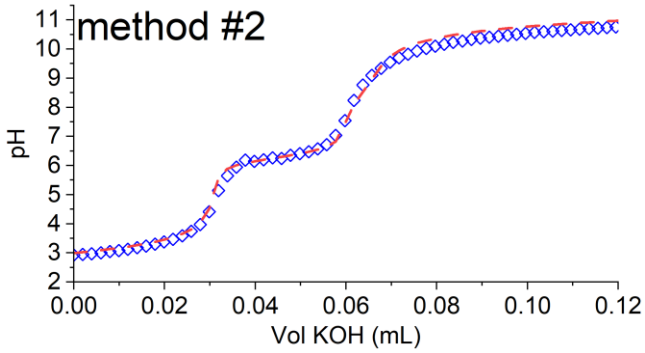
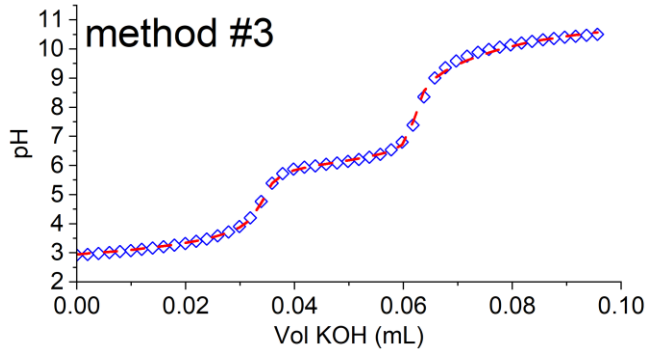	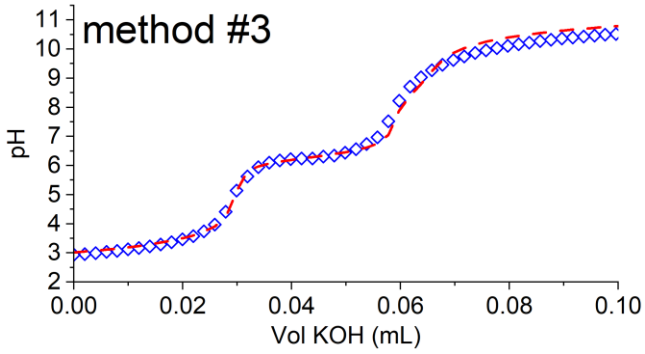

Figure S16 Potentiometric titration curve for complex-formation of **Nickel(II)-GGH-Pep** and **Nickel(II)-AAH-Pep**, acquired with Method #1, Method #2 and Method #3 at T = 298.15 K and I = 0.1 M (KCl). (Cu(II):Pep = 1:1.2, [Pep] = 0.3 mM, [Ni(II)]= 0.25 mM; KOH] = 0.04917 M). Blue diamonds: experimental data, red dotted line: fitting of potentiometric curve with the speciation model obtained with Method #3. Comparison of the pK_a obtained are reported in Table S4.

Table S4. Logarithms of overall formation constants (Log β) and acid dissociation constants (pK_a) of the Nickel(II) complexes of **GGH-Pep** and **AAH-Pep** in aqueous solution (T = 298.2 K, I = 0.1 M in KCl) obtained with reliable speciation model based on long equilibration time (Method #3) and underestimates constants which would otherwise be obtained without long enough equilibration time (Method #1 and Method #2). Standard deviations are given in parenthesis. L represents the completely deprotonated form of the peptide, and H_4L^{4+} the fully protonated **GGH-Pep** peptide and H_2L^{2+} the fully protonated **AAH-Pep** peptide.

		Potentiometric curve with spike (**Method #1**)			Potentiometric curve with spike (**Method #2**)			Reliable potentiometric curve (**Method #3**)		
GGH-Pep	Species	Log β		pK_a	Log β		pK_a	Log β		pK_a
	$[NiL]^{2+}$	11.9(1)		**8.9**	12.7		**9.2**	13.14(2)		**9.4**
	$[NiLH_{-1}]^{+}$	3(1)		**9.6**	3.5		**10.0**	3.7(1)		**10.0**
	$[NiLH_{-2}]$	−7.0(2)		--	-6.45		**--**	−6.25(7)		**--**
AAH-Pep	Species	Log β		pK_a	Log β		pK_a	Log β		pK_a
	$[NiLH_{-2}]$	-7.7(3)*		**7.4(6)***	-6.87(3)		**8.5(2)**	-7.37(5)		**8.8(3)**
	$[NiLH_{-3}]^{-}$	-15.1(7)*		**--**	-15.4(4)		**--**	-16.1(3)		**--**

* fitting not reliable, just an indicative value

1 N. L. Benoiton, *Chemistry of Peptide Synthesis*, CRC Press, Boca Raton, FL, 1st Editio., 2016.

2 W. C. Chan and P. D. White, *Fmoc Solid Phase Peptide Synthesis: A Practical Approach*, Oxford University Press, New York, 2000, vol. 222.

3 V. Borghesani, *Journal of Peptide Science*, 2024, **n/a**, e3649.

4 K. J. McKnelly, W. Sokol and J. S. Nowick, *J Org Chem*, 2020, **85**, 1764–1768.

5 R. Subirós-Funosas, R. Prohens, R. Barbas, A. El-Faham and F. Albericio, *Chemistry – A European Journal*, 2009, **15**, 9394–9403.

6 S. R. Manne, A. El-Faham, B. G. de la Torre and F. Albericio, *Tetrahedron Lett*, 2021, **85**, 153462.

7 N. A. Sole and G. Barany, *J Org Chem*, 1992, **57**, 5399–5403.

8 C. N. Pace, F. Vajdos, L. Fee, G. Grimsley and T. Gray, *Protein Science*, 1995, **4**, 2411–2423.

9 C. N. Pace and F. X. Schmid, in *Protein structure : a practical approach*, ed. T. E. Creighton, Oxford University Press, New York, 1997.

10 G. R. Grimsley and C. N. Pace, *Curr Protoc Protein Sci*, DOI:10.1002/0471140864.ps0301s33.

11 G. Gran, *Analyst*, 1952, **77**, 661–671.

12 P. Gans, A. Sabatini and A. Vacca, *Talanta*, 1996, **43**, 1739–1753.

13 L. Alderighi, P. Gans, A. Ienco, D. Peters, A. Sabatini and A. Vacca, *Coord Chem Rev*, 1999, **184**, 311–318.

14 M. Perinelli, R. Guerrini, V. Albanese, N. Marchetti, D. Bellotti, S. Gentili, M. Tegoni and M. Remelli, *J Inorg Biochem*, 2020, **205**, 110980.